A Phenomenological Model of a Reacting Fuel Jet Tilted in Crossflow Employing Air Entrainment

Wang K.[1], Fang J.[1,]*, Wang J.W.[1], Zheng S.M.[1], Shah H.R.[1], Guan J.F.[2], Lin S.B.[1], Zhang Y.M.[1]

[1] *University of Science and Technology of China, State Key Laboratory of Fire Science, Hefei, Anhui, China*
[2] *Tsinghua University, Hefei Institute for Public Safety Research, Hefei, Anhui, China*
**Corresponding author's email: fangjun@ustc.edu.cn*

ABSTRACT

Jet flame combustion in cross-flow is meaningful to promote reaction in many industrial combustion devices. Previous research about the tilt angle has limited predictive capability in a large range of the jet-to-crossflow momentum flux ratio (R_M). In this work, a new tilt angle model was provided by employing the air entrainment. The study showed that: the air entrainment ratio, defined as the mass flow rate ratio of the hot gas in the whole flame region to stoichiometric gases, was neversely proportional to the jet flame Froude number (Fr). Additionally, two regimes of the tilt angles were identified as $1 < Fr < 10^3$, $0.1 < R_M < 100$ for medium turbulent jet flames, and $10^3 < Fr < 10^6$, $100 < R_M < 3000$ for highly turbulent jet flames, respectively. For a fixed Fr, with the increasing R_M, the tilt angle decreased. For highly turbulent jet flames, the contributions of air entrainment to the tilt angle could be ignored; with the same R_M value, the flame deflected more than the low momentum jet flames.

KEYWORDS: Turbulent diffusion flame, cross-flow, tilt angle, momentum flux ratio, air entrainment.

NOMENCLATURE

b	Flame half-width
C_f	Drag coefficient
d_n	Nozzle diameter
Fr	Froude number $Fr = u_j^2/(gd_n)$
L	Length
$\dot{m}_{air}$, $\dot{m}_j$	Mass flow rate of entrained air or fuel jet
$\dot{m}_H$, $\dot{m}_V$	Mass flow rate in the horizontal or vertical direction
MW	Molecular weight
r	Radial direction
Re	Renolds number $\mathrm{Re} = \rho_j u_j d_n/\mu_j$
Ri	Richardson number $\mathrm{Ri} = (\rho_\infty - \rho_f) g d_n / (\rho_f u_j^2)$
x, z	Cartesian coordinates

Greek

$\alpha_{e(\dot{m})}$	Mass flow rate ratio of hot gases in the whole flame region to stoichiometric gases
θ	Flame tilt angle
μ	Dynamic viscosity
ξ	Axial ordinate in x, z plane
ρ	Density
σ	Standard deviation

Subscripts

ad	Adiabatic condition
air	Air
j	Fuel jet
f	Flame

Proceedings of the Ninth International Seminar on Fire and Explosion Hazards (ISFEH9), pp. 851-859
Edited by Snegirev A., Liu N.A., Tamanini F., Bradley D., Molkov V., and Chaumeix N.
Published by Saint-Petersburg Polytechnic University Press
ISBN: 978-5-7422-6498-9 DOI: 10.18720/spbpu/2/k19-93

R_M Jet-to-crossflow momentum flux ratio

$R_M = (\rho_j u_j^2)/(\rho_\infty u_w^2)$

S Air-to-fuel mass stoichiometric ratio

T Temperature

u Velocity

H, V Horizontal or vertical direction

N_2 Nitrogen

st Stoichiometric condition

w Wind

∞ Ambient condition

INTRODUCTION

The jet in cross-flow or transverse jet has been studied extensively because of its relevance to a wide variety of flows in technological systems, including fuel or dilution air injection in gas turbine engines, thrust vector control for high speed air breathing and rocket vehicles, and exhaust plumes from power plants [1, 2]. In practical engineering, researches relating to the tilt behavior of the momentum controlled jet flame in cross-flow are very important combustion design.

Escudier [3] presented a theoretical treatment for the motion of a turbulent gas jet burning in an oxidizing crossflow. Brzustowski [4] described a simple model of a hydrocarbon turbulent diffusion flame in a horizontal subsonic cross-flow of air and modeled the flame as a bent-over initially vertical and non-buoyant circular jet. Kostiuk et al. [5] changed the traverse air velocity and diameter of the burner tube to consider the scaling of the flame length, the cross-stream dimension of the plume of combustion products, and the overall combustion efficiency of wake-stabilized jet diffusion flames. Zhao et al. [6] gave a correlation for the stoichiometric flame length in crosswind as a function of the fuel source Froude number and the velocity ratio of wind to fuel based on the numerical results. Huang et al. [7] found that there are four ranges of flame pulsation intensities: slight, medium, strong, and over excitations. Besides, Hu and his co-workers have produced a series of experiments to study the flame tilt angle [8, 9], horizontal extents [10], flame length evolution [11] etc of diffusion flames under cross-wind. Recently, Tang et al. [12] studied the flame base drag length of diffusion flames with different aspect ratios under crossflow.

For the flame tilt angle, Pipkin et al. [13] deduced a classical model, in which cylindrical flame shape was assumed, the fuel velocity was expected to be uniform in the visible flame region. Flame width has the same size with the pool diameter, and the wind was assumed to have a 'drag force' with a drag coefficient C_f. When the momentum balance due to the cross-wind, initial inertia and buoyancy was applied in the direction normal to the surface of the flame body (positive upward), the tilt angle θ was:

$$f(\theta) = \frac{\tan\theta}{\cos\theta} = \frac{2C_f}{\pi} \frac{1}{1+Ri\left(\rho_f/\rho_j\right)\cos\theta} \frac{\rho_\infty u_w^2 L_f}{\rho_j u_j^2 d_n}, \tag{1}$$

where the Richardson number is $\mathrm{Ri} = (\rho_\infty - \rho_f) g d_n / (\rho_f u_j^2)$, ρ is the density, u is the velocity, L is the length, d_n is the nozzle diameter. The subscripts f, j, w, ∞, 0 represent flame, fuel jet, cross-flow, ambient condition, and initial condition, respectively. It can be seen that, the title angle is dependent on the flame length, the drag coefficient C_f depends on multiple factors and is very complicated to be interpreted and obtained. Moreover, the effects of entrained air have been ignored.

In the previous work, the tilt angle mainly depends on the flame length and other unpredictable parameters [13], or the air entrainment was assumed to be of a value that only supports complete combustion [14]. However, in the cross-wind condition, a large amount of air was entrained into the flame convection zone and the flame upper edge by coherent structures with large vortices, leading to great variation in the flame tilt angle [15]. Therefore, the variation of air entrainment can greatly affect the flame inclination, which cannot be neglected, or assumed to be of fixed valued.

In the present work, the tilt angle of momentum-controlled highly turbulent jet flames was modelled by employing air entrainment, which was different from the model of Eq. (1) that depends on unpredicatable parameters, and previous work [14] in which the air entrainment ratio was assumed to be unity. Experiments of momentum-controlled propane jet flames with values of R_M of 0.1–10, Fr of 1–100 were carried out in a open-loop wind tunnel, in order to verify the tilt angle model.

THEORETICAL ANALYSIS

Assumption made in building the model are: the diffusion flame is axisymmetric [4], steady and isothermal; the cross-flow is steady and non-turbulent; the cylindrical flame has an average flame width [16]; self-similarity of the jet flame is retained in cross-flow; stoichiometric and fast chemical reaction prevails; and the burning efficiency of the propane is assumed to be 100% [5].

Additionally, the buoyancy was neglected in this model. One might expect the vertical velocity to decrease by entrainment but increase by buoyancy simultaneously. Escudier [3] has pointed out that, buoyancy forces generated by the release of thermal energy during the combustion process have a negligible effect on the motion until far downstream. For highly turbulent jet flow, $Ri\left(\rho_f/\rho_j\right)\cos\theta$ in Eq. (1) is generally far smaller than unity, indicating that buoyancy momentum is small compared with inertia momentum. Furthermore, the solution of the effects of scaling on the relative influence of initial momentum and buoyancy showed that, due to the decrease of the vertical velocity, the flame bends over near the nozzle. Buoyancy has little influence near the nozzle, while it has a large influence in the downstream to curve up the flame [4].

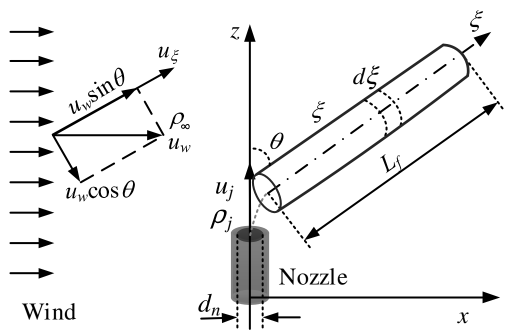

Fig. 1. Configurations of a tilted jet flame in cross-flow in x, z coordinates. (The gas jet discharges at a velocity u_j with density ρ_j from a nozzle of diameter d_n into a cross-flow of density ρ_∞ at horizontal velocity u_w; ξ is the axial ordinate in x, z plane; $d\xi$ is the flame element; $u_w \sin\theta$ and $u_w \cos\theta$ are the components of the cross-flow velocity, parallel and normal to the axial velocity u_ξ, respectively).

The definitions of the configuration of a tilted flame in cross-flow are shown in Fig. 1. When the momentum balance is applied in the direction of the main flow motion:

$$\tan\theta = \left(\dot{m}_H u_w\right)/\left(\dot{m}_V u_V\right). \tag{2}$$

Based on the assumption of a cylindrical flame shape, in the horizontal direction, the cross-flow mass flow rate through the cylindrical flame surface is:

$$\dot{m}_H = \rho_\infty u_w 2bL_f \cos\theta \,, \tag{3}$$

where b is the half-width of the flame.

For stoichiometric reaction, the air entrainment ratio $\alpha_{e(\dot{m})}$, i.e., the mass flow rate ratio of the hot gas in the whole flame region to stoichiometric gases, is:

$$\alpha_{e(\dot{m})} = \dot{m}_{air} \big/ \left((S+1)\dot{m}_j \right) . \tag{4}$$

Here S is the air-to-fuel mass stoichiometric ratio, $\dot{m}_{air}$ and $\dot{m}_j$ are the mass flow rates of entrained air and fuel jet, respectively. $\alpha_{e(\dot{m})}$ is related to the air entrainment coefficient [17], but not the same.

The mass flow rate of the mixture of stoichiometric gas and entrained air is $\dot{m}_V = \alpha_{e(\dot{m})}(S+1)\dot{m}_j$. Eq. (2) then becomes:

$$\tan\theta = \frac{\rho_\infty u_w^2 2bL_f \cos\theta}{\bar{\alpha}_{e(\dot{m})}(S+1)\dot{m}_j u_V} . \tag{5}$$

For a cylindrical flame, its tilt angle is constant. Here in the whole flame length L_f, there are three characteristic parameters are assumed: the air entrainment ratio $\bar{\alpha}_{e(\dot{m})}$, flame mean half-width $\bar{b}$, and vertical velocity $\bar{u}_V$. Altering the form of Eq. (5), gives:

$$\frac{\tan\theta}{\cos\theta} = \frac{\rho_\infty u_w^2 2\bar{b}L_f}{\bar{\alpha}_{e(\dot{m})}(S+1)\dot{m}_f \bar{u}_V} . \tag{6}$$

The solutions of $\bar{b}$ and $\bar{u}_V$ are now addressed.

The similarity solution for the flame half-width, b, relates to the axial coordinate by [18]:

$$b(\xi) = 0.23\xi\left(\rho_{st}/\rho_j\right)^{1/2} , \tag{7}$$

where $\rho_{st}/\rho_j = \left(MW_{N_2}/MW_j\right)\left(T_j/T_{st}\right)$, MW are the molecular weights, T is the temperature, the subscripts N_2 and st stand for the nitrogen gas and stoichiometric condition, respectively. For the case of a one-step irreversible reaction with infinitely fast chemistry, with assumed, infinitely fast, reversible, reactions are assumed, all species are in chemical equilibrium at each value of mixture fraction. If the enthalpy equation takes the same form as the mixture fraction, the enthalpy becomes a linear function of the mixture fraction. The stoichiometric temperature T_{st} calculated under these conditions is the adiabatic flame temperature T_{ad} [19]. With $T_{st} = T_{ad} = 1554$ K [20].

In the isothermal flame, the mean half-width in the flame region is:

$$\bar{b} = \frac{1}{L_f}\int_0^{L_f} b(\xi)d\xi = \frac{1}{2}b(L_f) = 0.115L_f\left(\rho_{st}/\rho_j\right)^{1/2} . \tag{8}$$

In still air, the axial velocity ($\xi = z$) can be obtained, based on Spalding's entrainment theory, [4]:

$$\frac{u_\xi(\xi)}{u_j(\xi)} = \left(1 + 0.32\left(\xi/d_n\right)\left(\rho_\infty/\rho_j\right)^{1/2}\right)^{-1} . \tag{9}$$

Here $u_\xi(\xi)$ is the axial velocity at ξ height and $u_j(\xi{=}0) = u_j$. With cross-flow, $u_\xi(\xi)$ is the axial velocity at ξ along ξ direction, $u_j(\xi)$ is the initial coupling velocity of jet and cross-flow in ξ direction.

The average velocity over the flame length $\bar{u}_\xi$ is then defined by assuming the same residence time is retained, as:

$$\frac{L_f}{\bar{u}_\xi} = \int_0^{L_f} \frac{1}{u_\xi(\xi)} d\xi . \tag{10}$$

Substituting Eq. (9) in Eq. (10), the flame axial velocity, averaged in the axial direction, $\bar{u}_{\xi(axial)}$ is:

$$\bar{u}_{\xi(axial)} = u_j(\xi)\left(1 + 0.16\left(L_f/d_n\right)\left(\rho_\infty/\rho_j\right)^{1/2}\right)^{-1} . \tag{11}$$

In the radial direction r of the flame, the vertical velocity distribution has the following form:

$$u_\xi(\xi, r) = u_\xi(\xi)\exp\left(-r^2/\left(2\sigma^2\right)\right), \tag{12}$$

where σ is the standard deviation related to the spread of the profile across the centerline. Since 4σ is the width of the distribution that encompasses 95% of the area under the profile from statistics, one can assume 4σ = 2b. Thus the average vertical velocity across the radial direction is:

$$\bar{u}_{\xi(radial)} = \frac{1}{\pi b^2}\int_0^\infty 2\pi r u dr = \frac{u_\xi(\xi)}{2} . \tag{13}$$

Combining Eqs. (11) and (13), the average fuel velocity in still air is:

$$\bar{u}_{\xi(axial,radial)} = \frac{1}{2} u_j(\xi)\left(1 + 0.16\left(L_f/d_n\right)\left(\rho_\infty/\rho_j\right)^{1/2}\right)^{-1} . \tag{14}$$

When there is cross-flow, as shown in Fig. 1, ξ becomes the flame tilt coordinate, $\xi\cos\theta = z$. The scalars of the vectors in ξ and $\xi\cos\theta$ (z) coordinates have the following mapping relationships:

$$\xi \to \xi\cos\theta = z,\ r \to r\cos\theta,\ \sigma \to \sigma\cos\theta,\ u_j(z) = u_j(\xi)\cos\theta = u_j,\ u_\xi(z) = u_\xi(\xi)\cos\theta . \tag{15}$$

Based on Eq. (15), the average vertical velocity at $L_f \cos\theta$ height in cross-flow is:

$$\bar{u}_V \approx \frac{1}{2} u_j\left(1 + 0.16\cos\theta\left(L_f/d_n\right)\left(\rho_\infty/\rho_j\right)^{1/2}\right)^{-1} . \tag{16}$$

Substituting Eqs. (8), (16) and $R_M = (\rho_j u_j^2)/(\rho_\infty u_w^2)$ into Eq. (6) gives:

$$\frac{\tan\theta}{\cos\theta}\left(1 + 0.16\cos\theta\left(L_f/d_n\right)\left(\rho_\infty/\rho_j\right)^{1/2}\right) = \frac{2}{\pi}\frac{1}{\bar{\alpha}_{e(\dot{m})}(S+1)R_M}\left(L_f/d_n\right)^2\left(\rho_{st}/\rho_j\right)^{1/2} . \tag{17}$$

In still air, experiments have shown that the length of a momentum-controlled turbulent diffusion flame is about 100d_n. The value of L_f/d_n is very large and Eq. (17) can be simplified:

$$\frac{\tan\theta}{\cos\theta}\left(0.16\cos\theta\left(L_f/d_n\right)\left(\rho_\infty/\rho_j\right)^{1/2}\right) = \frac{2}{\pi}\frac{1}{\bar{\alpha}_{e(\dot{m})}(S+1)R_M}\left(L_f/d_n\right)^2\left(\rho_{st}/\rho_j\right)^{1/2} . \tag{18}$$

For low Mach number flow jets, Fr numbers are generally smaller than 10^5. The inclined flame length ratio L_f/d_n is independent of the momentum ratio [21]. The theoretical and experimental results showed that, the dimensionless heights of turbulent flames are dependent on Fr as $L_f/d_n = 27Fr^{1/5}$ [18], With

$\frac{\rho_\infty}{\rho_j} = \frac{MW_{\text{air}}}{MW_j}\frac{T_j}{T_\infty}$, $\frac{\rho_{st}}{\rho_j} = \frac{MW_{\text{N}_2}}{MW_j}\frac{T_j}{T_{st}}$, $T_j = T_\infty$, $MW_{\text{air}} \approx MW_{\text{N}_2}$, Eq. (18) can be further simplified to give:

$$\tan\theta = \frac{337.5}{\pi}\frac{1}{\bar{\alpha}_{e(\dot{m})}(S+1)R_M}\left(T_\infty/T_{st}\right)^{1/2} Fr^{1/5} . \tag{19}$$

According to the definition of $\bar{\alpha}_{e(\dot{m})}$ in Eq. (4), when $\bar{\alpha}_{e(\dot{m})} \le 1$, the amount of entrained air is less than required for stoichiometric combustion, which is very common for the high speed, strong jet flame. When $\bar{\alpha}_{e(\dot{m})} > 1$, it implies that a large amount of air, sufficient to cause oxygen-rich combustion, is entrained into the flame, which occurs for low speed jet flames.

EXPERIMENTAL SETUP

Propane was used as the fuel and all experiments were carried out in a wind tunnel with a test section 6 m long, 1.8 m wide and 1.8 m high. The facility can simulate cross-flow between 0.5 and 15 m/s with turbulence fluctuation intensity of less than 2%. The transient cross-flow is measured by four hot-wire anemometers, with an accuracy of 0.01 m/s.

Four nozzle sizes were used with inside diameters from 8 to 14 mm, and the nozzle, in the middle of the test section, at a height of 50 cm, to reduce the influence of the floor boundary layer. The vertical jet flow was measured and controlled by an Alicat mass flow meter, with a precision of ±(0.8% of reading + 0.2% of full scale).

The jet-to-crossflow momentum flux ratio R_M for this work was in the range of 0.1~10, where the Reynolds number ($\mathrm{Re} = \rho_j u_j d_n/\mu_j$, and Froude number $Fr = u_j^2/(gd_n)$ of the jet fuel gas are approximately $2100 < Re < 4000$ and $1 < Fr < 100$.

A high speed camera (2000 frames per second) was used in the front perspective of the tilted flames to record video images through the glass observation window on the side of the wind tunnel [14].

RESULTS AND DISCUSSION

Imaging analysis

Figure 2 shows typical flame images recorded by the high speed camera (a) and the contours of flame intermittent rate (b). In Fig. 2, the flickering flame length was obtained by image processing and the flame tilt angle by the vector of the mean flame length. The slant length was defined as the distance between the center of the nozzle exit and the “peak” of the contour of fifty percent of flame occurrence probability. With increasing wind velocity, the flame was increasingly inclined from the nozzle axis.

Tilt angle regime

The tilt angle with different Froude numbers, air entrainment ratio, and various momentum flux ratios, over a large range is shown in Fig. 3.

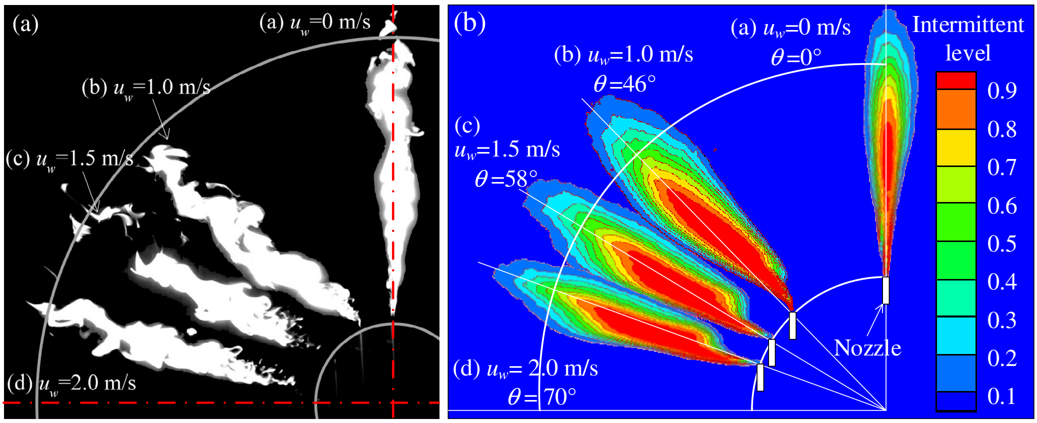

Fig. 2. Flame images (a) and the contours of the flame intermittent rate (d_n = 8 mm, u_j = 2.65 m/s).

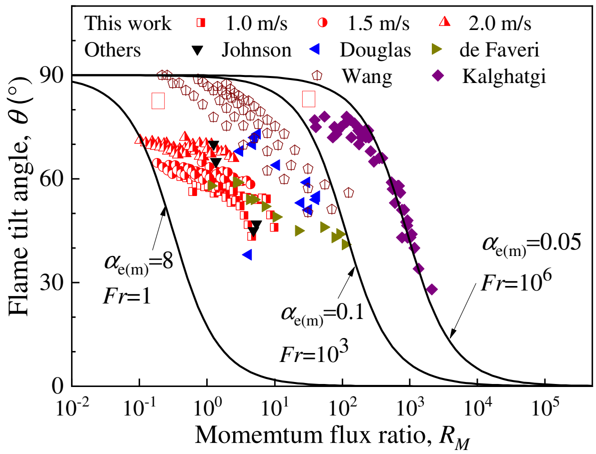

Fig. 3. Tilt angle with momentum flux ratio. The solid line is based on Eq. (19). Johnson [22]: propane, methane, 18.8 < Fr < 20.3; Douglas [23]: flare stack, 25 < Fr < 59; de Faveri [24]: diesel oil, 0.085 < Fr < 1.36; Kalghatgi [25]: propane, 1022 < Fr < 6.7×10^5; Wang [26]: propane, 47 < Fr < 756.

Escudier [3] postulated that the air is entrained into the jet at rates proportional to the magnitudes of these two characteristic velocities by using Morton entrainment theory, which can be expressed as:

$$d\dot{m}_{air}/d\xi = 2\pi\rho_\infty b\left(\alpha_{e(u)}\left|u_\xi - u_w\sin\theta\right| + \beta_{e(u)}u_w\cos\theta\right), \quad (20)$$

where $\alpha_{e(u)}, \beta_{e(u)}$ are the air entrainment coefficients related to the components of the cross-flow velocity parallel and normal to the flame axis. Ricou and Spalding [27] showed that for large ξ/d_n, $\alpha_{e(\dot{m})} = \dot{m}_{air}/(S+1)\dot{m}_j \propto \xi$, and $\alpha_{e(\dot{m})} = 0$ at ξ = 0. After dividing Eq. (20) by the fuel mass flow rate $\dot{m}_j = \pi d_n^2 u_j \rho_j/4$, the universal excess air entrainment ratio in the flame region is:

$$\bar{\alpha}_{e(\dot{m})} = \frac{d\alpha_{e(\dot{m})}}{d\xi}L_f = 8\frac{1}{S+1}\frac{L_f b}{d_n^2}\left(\frac{\rho_\infty}{\rho_j}\right)\left[\bar{\alpha}_{e(u)}\left(\frac{\left|\bar{u}_\xi - u_w\sin\theta\right|}{u_j}\right) + \bar{\beta}_{e(u)}\frac{u_w\cos\theta}{u_j}\right]. \quad (21)$$

As $Fr = u_j^2 / (g d_n)$, $\bar{\alpha}_{e(\dot{m})} \sim 1/Fr$. Therefore, the values of $\bar{\alpha}_{e(\dot{m})}$ and Fr in the calculation of the solid line in Fig. 3 were negatively correlated with each other.

There are two regimes (regime I: $1 < Fr < 10^3$, $0.1 < R_M < 100$; regime II: $10^3 < Fr < 10^6$, $100 < R_M < 3000$) for the medium and highly turbulent jet flames, respectively. For fixed Froude numbers, with increasing R_M, the tilt angles decreases. For highly turbulent jet flames in regime II, as the jet-flow Froude number is very large, the contributions of air entrainment to the tilt angle is negligible, so with the same R_M, the tilt angle is bigger than the low momentum jet flames in regime I.

CONCLUSIONS

Motivated by improving the understanding of the behaviors of jet flame in cross-flows, the work has provided a new tilt angle equation for air entrainment. The air entrainment ratio, defined as the mass flow rate ratio of the hot gas in the whole flame region to stoichiometric gases, was proportional to the jet flame Fr.

Experiments with propane jet diffusion flames analyzed and verified the angle equation. Based on the experimental results and tilt angle equation, two regimes of tilt angles were identified for the medium and highly turbulent jet flames: regime I: $1 < Fr < 10^3$, $0.1 < R_M < 100$; regime II: $10^3 < Fr < 10^6$, $100 < R_M < 3000$. For fixed Froude numbers, with increasing R_M, the tilt angle decreased. For highly turbulent jet flames, the contributions of air entrainment to the tilt angle can be ignored, so with the same R_M value, the flame deflected more than in low momentum jet flames.

ACKNOWLEDGMENTS

This work was sponsored by the National Natural Science Foundation of China (Nos. 51636008, 51576186, and 51323010), Key Research Program of the Chinese Academy of Sciences (No. QYZDB-SSW-JSC029), National Key R&D Program (No. 2016YFC0801500), Fundamental Research Funds for the Central Universities (No. WK2320000036) and China Postdoctoral Science Foundation funded project (No. 2018M632549). Fang Jun expresses sincere appreciation to Prof. Forman A. Williams for his valuable suggestions during the visit to UCSD.

References

[1] A.R. Karagozian, Transverse jets and their control, Prog. Energy Combust. Sci. 36 (2010) 531-553.

[2] L. Hu, A review of physics and correlations of pool fire behaviour in wind and future challenges, Fire Saf. J. 91 (2017) 41-55.

[3] M.P. Escudier, Aerodynamics of a burning turbulent gas jet in a crossflow, Combust. Sci. Technol. 4 (1971) 293-301.

[4] T.A. Brzustowski, The hydrocarbon turbulent diffusion flame in subsonic cross-flow, In. The hydrocarbon turbulent diffusion flame in subsonic cross-flow. Los Angeles, California, 1977, pp. 24-26.

[5] L.W. Kostiuk, A.J. Mejeski, P. Poudenx, M.R. Johnson, and D.J. Wilson, Scaling of wake-stabilized jet diffusion flames in a transverse air stream, Proc. Combust. Inst. 28 (2000) 553-559.

[6] Y. Zhao, L. Jianbo, and L. Lu, Numerical modeling of fires on gas pipelines, Appl. Therm. Eng. 31 (2011) 1347-1351.

[7] R.F. Huang, R.K. Kimilu, and C.M. Hsu, Effects of jet pulsation intensity on a wake-stabilized non-premixed jet flame in crossflow, Exp. Therm. Fluid Sci. 78 (2016) 153-166.

[8] X. Zhang, W. Xu, L. Hu, X. Liu, X. Zhang, and W. Xu, A new mathematical method for quantifying trajectory of buoyant line-source gaseous fuel jet diffusion flames in cross air flows, Fuel 177 (2016) 107-112.

[9] F. Tang, L. Hu, X. Zhang, X. Zhang, and M. Dong, Burning rate and flame tilt characteristics of radiation-controlled rectangular hydrocarbon pool fires with cross air flows in a reduced pressure, Fuel 139 (2015) 18-25.

[10] Y. Lin, X. Zhang, and L. Hu, An experimental study and analysis on maximum horizontal extents of buoyant turbulent diffusion flames subject to relative strong cross flows, Fuel 234 (2018) 508-515.

[11] Q. Wang, L.H. Hu, X. Zhang, X. Zhang, S. Lu, and H. Ding, Turbulent jet diffusion flame length evolution with cross flows in a sub-pressure atmosphere, Energy Convers. Manage. 106 (2015) 703-708.

[12] F. Tang, Q. He, and J. Wen, Effects of crosswind and burner aspect ratio on flame characteristics and flame base drag length of diffusion flames, Combust. Flame 200 (2019) 265-275.

[13] O.A. Pipkin, and C.M. Sliepcevich, Effect of Wind on Buoyant Diffusion Flames. Initial Correlation, Ind. Eng. Chem. Fund. 3 (1964) 147-154.

[14] J.W. Wang, J. Fang, S.B. Lin, J.F. Guan, Y.M. Zhang, and J.J. Wang, Tilt angle of turbulent jet diffusion flame in crossflow and a global correlation with momentum flux ratio, Proc. Combust. Inst. 36 (2017) 2979-2986.

[15] M. Tsue, T. Kadota, and M. Kono, Temperature and velocity fluctuations of a jet diffusion flame in a cross-flow, Proc. Combust. Inst. 29 (2002) 1937-1942.

[16] A.J. Majeski, D.J. Wilson, and L.W. Kostiuk, Predicting the Length of Low-Momentum Jet Diffusion Flames in Crossflow, Combust. Sci. Technol. 176 (2004) 2001-2025.

[17] B. Karlsson, J. Quintiere, Enclosure Fire Dynamics, CRC Press, 2000.

[18] N. Peters, Turbulent Combustion, Cambridge University Press, Cambridge, U.K., 2004.

[19] N. Peters, Turbulent Combustion, Cambridge University Press, Cambridge, U.K., 2004.

[20] M.J. Hurley, D.T. Gottuk, J.R. Hall Jr, K. Harada, E.D. Kuligowski, M. Puchovsky, J.M. Watts Jr, and C.J. Wieczorek, SFPE Handbook of Fire Protection Engineering, (5th ed), Springer, 2015.

[21] P.J. DiNenno, SFPE Handbook of Fire Protection Engineering, (3rd ed), National Fire Protection Association, Quincy, MA, 2002.

[22] M.R. Johnson, and L.W. Kostiuk, Efficiencies of low-momentum jet diffusion flames in crosswinds, Combust. Flame 123 (2000) 189-200.

[23] D.M. Leahey, and M.B. Schroeder, Observations and predictions of jet diffusion flame behaviour, Atmos. Environ. 21 (1987) 777-784.

[24] D.M. de Faveri, A. Vidili, R. Pastorino, and G. Ferraiolo, wind effects on diffusion flames of fires of high source momentum, J. Hazard. Mater. 22 (1989) 85-100.

[25] G.T. Kalghatgi, The visible shape and size of a turbulent hydrocarbon jet diffusion flame in a cross-wind, Combust. Flame 52 (1983) 91-106.

[26] J. Wang, J. Fang, J. Guan, Y. Zhang, and J. Sun, Effect of crossflow on the air entrainment of propane jet diffusion flames and a modified Froude number, Fuel 233 (2018) 454-460.

[27] F.P. Ricou, and D.B. Spalding, Measurements of entrainment by axisymentrical turbulent jets, J. Fluid Mech. 11 (1961) 21-32.